

## **The Advanced Camera for the Hubble Space Telescope**

Holland Ford, Paul Feldman, David Golimowski, Zlatan Tsvetanov

Department of Physics and Astronomy, Johns Hopkins University, Baltimore, Maryland 21218

Frank Bartko

Bartko Science and Technology, P.O. Box 26085, Highland Ranch, Colorado 80126-0858

Jim Crocker

European Space Observatory, Karl-Schwarzschild-str. 2, Garching bei Munchen, D85748, Germany

Pierre Bely, Robert Brown, Chris Burrows, Mark Clampin, George Hartig,  
Marc Postman, Marc Rafal, William Sparks, Rick White

Space Telescope Science Institute, 3700 San Martin Drive, Baltimore, Maryland 21218

Thomas Broadhurst

Department of Astronomy, University of California, Berkeley, California 94720

Garth Illingworth

Lick Observatory, University of California, Santa Cruz, California 95064

Tim Kelly, Bob Woodruff

Ball Aerospace Corporation, P.O. Box 1062, Boulder, Colorado, 80306-062

Edward Cheng, Randy Kimble, Carolyn Krebs, Susan Neff

NASA Goddard Space Flight Center, Greenbelt, Maryland 20771

Michael Lesser

Steward Observatory, University of Arizona, Tucson, Arizona 85721

George Miley

Leiden University, Sterrewacht Leiden, Nielsbohrweg 2, P.O. Box 9513, Leiden 2300A, The Netherlands

### **ABSTRACT**

The *Advanced* Camera for the Hubble Space Telescope will have three cameras. The first, the Wide Field Camera (WFC), will be a high throughput (45% at 700 nm, including the HST optical telescope assembly (OTA)), wide field (200''×204''), optical and I-band camera that is half critically sampled at 500 nm. The second, the High Resolution Camera (HRC), is critically sampled at 500 nm, and has a 26''×29'' field of view and 25% throughput at 600 nm. The HRC optical path will include a coronagraph which will improve the HST contrast near bright objects by a factor of ~10. The third camera is a far ultraviolet, Solar-Blind Camera (SBC) that has a relatively high throughput (6% at 121.6 nm) over a 26''×29'' field of view. The Advanced Camera for Surveys (ACS) will increase HST's capability for surveys and discovery by at least a factor of ten.

The ACS must be built in approximately one-third the time and for one quarter of the cost of the first and second generation HST instruments. There are three components of our strategy to achieve this demanding goal. The first is reliance on the design and technology of three previous HST instruments, STIS, NICMOS, and COSTAR. The second component is a strongly integrated team consisting of the Johns Hopkins University and the ACS Science Team, the Goddard Space Flight Center, and Ball Aerospace. The final aspect of ACS cost control is the science team’s philosophy of “keep it simple”. We prioritize our science goals and balance technical decisions on cost and performance against our most important science goals.

The ACS science team will use ~75% of its dedicated time to make a deep survey of ~ 3/4 of a square degree of sky. We expect to map the large-scale distribution of dark matter around approximately 20 rich clusters of galaxies. The survey data will establish the evolution of galaxies and clusters of galaxies in the early universe and determine the cluster and supercluster environment around one or more high redshift radio galaxies. In a second survey, we will use Surface Brightness Fluctuations (SBF) in deep WFC I-band images of early type galaxies to map large-scale flow. This method will allow us to obtain distances to galaxies which are independent of their redshifts and will contribute to the measurement of  $H_0$  and to the mapping of large-scale flows. We will use narrow band and polarimetric HRC and WFC images to address QSOs and AGNs, our second major science area. We will use a novel polarimetric technique to measure geometric distances to galaxies, and provide independent measures of  $H_0$  and  $q_0$ . A variety of observations using narrow band imaging with the SBC will address specific questions in solar system science. The coronagraph will be used to study the narrow line regions close the nuclei of active galaxies and the host galaxies of quasars. We will use the coronagraph to search nearby stars for proto-planetary disks, brown dwarf companions, and planets.

### 1. DESIGN PHILOSOPHY FOR THE ADVANCED CAMERA

We are building an *Advanced* Camera for the Hubble Space Telescope which will have a high throughput, wide field, optical and I-band camera (WFC), a critically sampled high resolution camera (HRC), and a high throughput, moderate field of view far ultraviolet, solar-blind camera (SBC). The Advanced Camera for Surveys (ACS) will increase HST’s capability for surveys and discovery by at least a factor of 10. The key characteristics of the ACS are listed in Table 1. We have included the FOC (Faint Object Camera) and WFPC2 (Wide Field Planetary Camera 2) for comparison.

Table 1: Key Characteristics of the Advanced Camera for Surveys

| Prioritized Features                  | WFC       |              | HRC       |              | SBC          |                   |
|---------------------------------------|-----------|--------------|-----------|--------------|--------------|-------------------|
|                                       | ACS WFC   | WFPC2 f/12.9 | ACS HRC   | WFPC2 f/28.3 | ACS SBC      | FOC* COSTAR f/151 |
| Max. throughput including HST OTA (%) | 45@700 nm | 14@600 nm    | 25@600 nm | 14@600 nm    | 6.1@121.6 nm | 1.6@**150 nm      |
| at 800 nm                             | 36        | 6.6          | 14        | 6.6          | 6.1@121.6 nm | 0.81@121.6 nm     |
| at 400 nm                             | 34        | 5.3          | 20        | 5.3          | 5.3@130 nm   | 1.3@130 nm        |
| at 200 nm                             | ---       | 0.012        | 12        | 1.2          | 4.1@140 nm   | 1.4@140 nm        |
|                                       |           |              |           |              | 2.9@150 nm   | 1.6@150 nm        |
|                                       |           |              |           |              | 1.7@160 nm   | 1.5@160 nm        |
| Equiv. field of view                  | 200"×204" | 143"×143"    | 26"×29"   | 35"×35"      | 26"×29"      | 7"×7"             |
| Sampling at 500 nm                    | Half      | Quarter      | Full      | Half         | Half***      | Full              |
| Polarization from design and coating  | <1%       | ~5%          | <5%       | ~5%          | <1%          | <1%               |

\*The FOC is not solar blind; \*\*Maximum in the FUV; \*\*\*@295 nm

Our approach to the ACS design was driven by two facts. First, images obtained with the FOC/COSTAR and WFPC2 cameras demonstrate that HST can deliver superb spatial resolution. Second, HST imaging with the present cameras is seriously limited by low throughputs (FOC and WFPC2), small fields of view (FOC), and undersampling (WFPC2). These three factors work together to severely limit HST’s utility for deep, high-resolution imaging and for deep surveys. The time required to survey an area of the sky to a given limiting magnitude and a specified signal-to-noise ratio (SNR) is inversely proportional to product of

the detector area and the net DQE when the SNR is limited by shot noise in the signal. When the SNR is limited by the shot noise in the background, the time is inversely proportional to  $\text{Area} \times \text{DQE}^2$ . The most conservative measure of HST's survey or discovery efficiency is thus  $\text{Area} \times \text{DQE}$ . We aim to improve HST survey efficiency in the optical, the far ultraviolet, and especially the I-band, by at least a factor of 10. To achieve this goal we paid careful attention to: i) an optical design that minimizes the number of reflections, ii) high reflectivity coatings on the mirrors, filters, and windows, and iii) obtaining CCDs with high quantum efficiency in the optical and the near infrared for the WFC, and in the near ultraviolet and optical for the HRC.

The ACS must be built in approximately one-third the time and for one quarter of the cost of the first and second generation HST instruments. Our primary strategy for building the ACS within the cost and schedule constraints set out in the NASA Announcement of Opportunity is reliance on the Space Telescope Imaging Spectrograph (STIS) design and technology. The SBC and HRC detectors and electronics are STIS design, and, in fact, for the SBC likely will be a STIS flight spare. The two  $2k \times 4k$  WFC I-band detectors and electronics derive directly from STIS CCDs. Whenever possible, we use STIS electronics and STIS mechanisms. Approximately 70% of our electronics modules and mechanisms are "build to print" from STIS drawings. The ACS flight software derives from STIS and NICMOS software whenever possible and practical.

The second aspect of cost control is a strongly integrated team consisting of the Johns Hopkins University and the ACS Science Team, the Goddard Space Flight Center, and Ball Aerospace. This ACS team minimizes management costs and maximizes scientific, managerial, and engineering resources which can be applied to building the ACS.

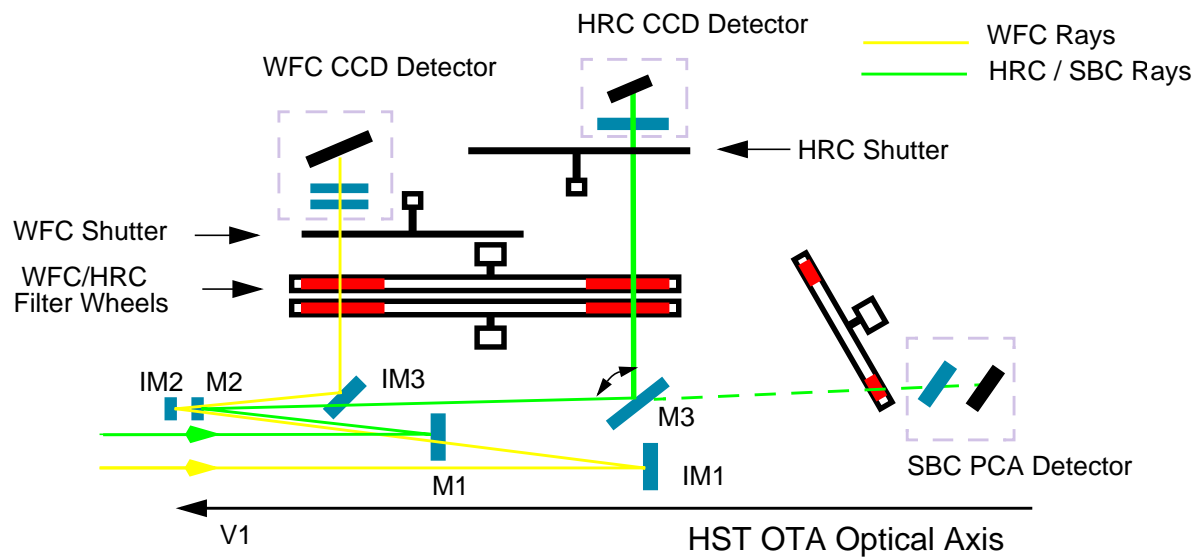
The final aspect of ACS cost control is the science team's philosophy of "keep it simple". We prioritize our science goals and balance technical decisions on cost and performance against our most important science goals. We are not trying to achieve the unrealistic goal of building an Advanced Camera that will do everything for everyone.

## 2. INSTRUMENT DESIGN

### 2.1 Overview of the Advanced Camera

Figure 1 shows the optical layout of the ACS. Figure 2 shows the layout of the ACS optical bench. The WFC and HRC have separate optical paths and mirrors. The WFC mirrors are designated IM1, IM2, and IM3. The HRC mirrors are designated M1, M2, and M3. The light in each optical path first encounters a spherical mirror (IM1 or M1) which images the HST pupil onto the IM2 (M2) mirror. These mirrors are anamorphic aspheres which are figured with the inverse spherical aberration on the HST primary mirror, and thus correct the spherical aberration in the HST primary and the field dependent astigmatism of the HST at the center of the ACS field of view. The light from the WFC IM2 mirror is reflected by a Schmidt-like plate (IM3) through the two filter wheels to the WFC CCDs. The Schmidt plate corrects astigmatism over the WFC field of view (FOV).

Fig. 1: An optical schematic of the Advanced Camera



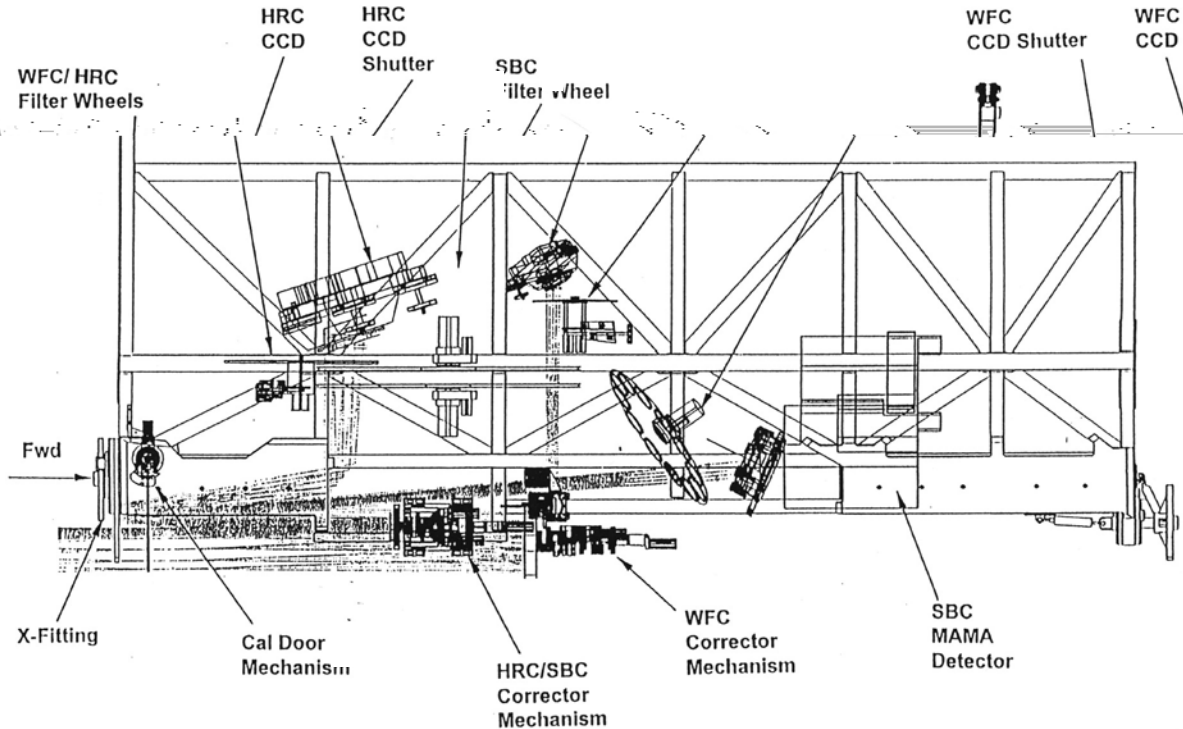


Fig. 2: The layout of the ACS optical bench

The HRC and the SBC use the same M1 and M2 mirrors. The  $MgF_2$  overcoatings on these two aluminum-coated mirrors are optimized for maximum reflectivity at 121.6 nm. Because of reflection losses in the far UV, we chose to have only two reflections in the optical path to the SBC. A flat mirror M3 is inserted into the light path to direct the light through the two filter wheels to the HRC 1024<sup>2</sup> CCD. The  $MgF_2$  coating on M3 is optimized for maximum reflectivity at wavelengths > 200 nm.

## 2.2 The Wide Field Camera

The WFC features a 200'' $\times$ 204'' field of view optimized for sky-limited V and I-band imaging. The WFC employs two butted SITE 2048 $\times$ 4096 CCDs with 15 micron pixels, with a plate scale of 0.051''/pixel and near critical sampling in the I-band. The expected characteristics of the CCDs are given in Table 2. The WFC high red throughput is achieved by a unique optical design employing only three mirrors with protected silver coatings, and the use of thinned, backside-illuminated CCDs with anti-reflection coatings optimized for red wavelengths. The reflectivity of three silver coated mirrors is 50 percent higher than three aluminum coated mirrors would be at 800 nm. The mirror coating as well as the geometry yield less than one percent polarization sensitivity. Figure 3 shows the expected reflectivity as a function of wavelength for overcoated silver mirrors. Overcoated silver mirrors maintain high reflectivity for several years with exposure to typical laboratory air quality and humidity.

Table 2: WFC Throughput and Noise Performance Requirements (excluding the OTA)

|   | Requirement | Goal | Predicted   |
|---|-------------|------|-------------|
| Minimum camera throughput at cold operating temperatures at:  |             |      |             |
| 450 nm  | 0.64        | 0.67 | 0.60/0.50   |
| 800 nm  | 0.59        | 0.68 | 0.60/0.81   |
| 1000 nm   | 0.1         | 0.17 | 0.11/0.09   |
| Minimum peak throughput                                       | 0.74        | 0.77 | 0.73/0.84   |
| Integration time for system noise performance per pixel (min) | 21          | 21   | 21          |
| RMS noise per pixel   | <5.8        | <4.6 | 5.8/4.4     |
| Flat field non-uniformity                                     | $\pm 10\%$  |      |             |
| Dynamic range per pixel over the entire CCD (full well/5.8)   | >8,620      |      | 8620/10,870 |

We have specified that the quantum efficiency (QE) at 800 nm must be  $\geq 59\%$ , with a goal of 68%. The maximum peak throughput must be  $\geq 74\%$  with a goal of 77%. Figure 4 shows the expected quantum efficiency of the WFC CCDs, and Figure 5 shows the expected net throughput of the WFC and the HRC, including the HST primary and secondary mirrors. For comparison, we have shown the net throughput of the WFPC2.

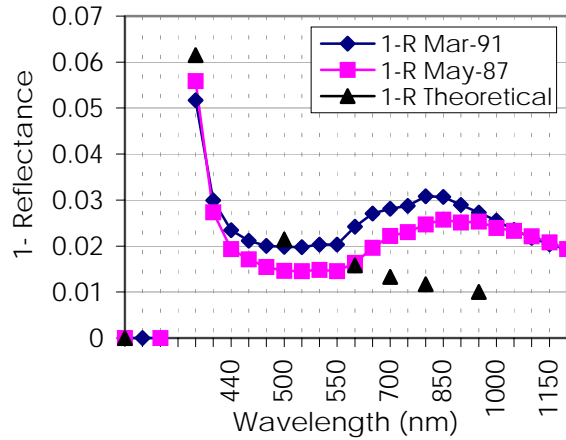


Fig. 3: Reflectance for overcoated silver

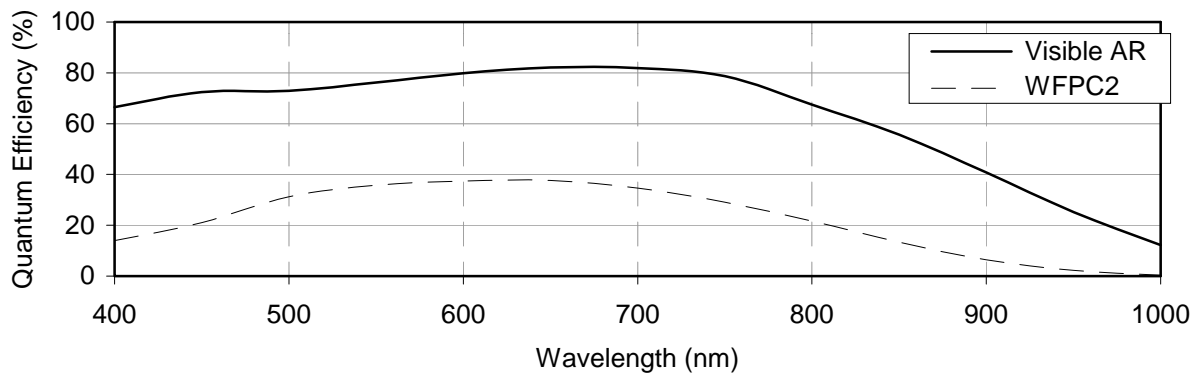


Fig. 4: The expected WFC CCD quantum efficiency with the standard SITE visible AR coating compared to the WFPC2 QE.

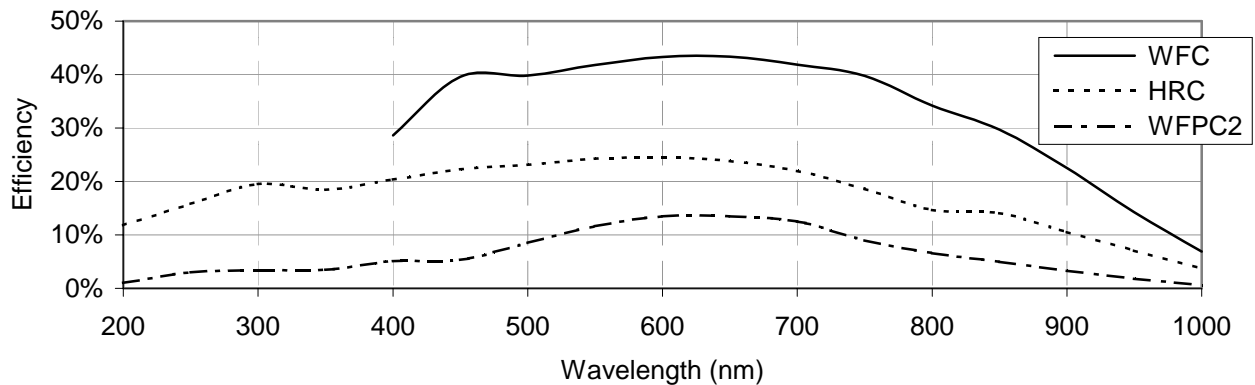


Fig. 5: The expected WFC and HRC net efficiencies (including the HST OTA) compared to the WFPC2.

### 2.2.1 Wide Field Camera Optics

The overall areal FOV is greater than 40,000 square arc sec. The WFPC2 Planetary Camera has a comparable resolution to the ACS WFC, but covers an areal FOV of 1,172 square arc sec, which is only 2.9 percent of the ACS WFC FOV. The relay optics, being all reflective, are fully corrected for color and correct the HST spherical aberration and astigmatism with a STIS type corrector. The relayed image is nearly free of all third-order aberrations except distortion and an acceptable amount of curvature of field. The spherical first corrector mirror (IM1) images the HST primary mirror onto the second corrector mirror. The second corrector mirror (IM2), an anamorphic asphere, is similar to the M2 mirror in COSTAR. It corrects the HST spherical aberration by compensating for the conic constant error of the primary mirror. The anamorphic shape of this mirror corrects the HST field-dependent astigmatism at the center of the field. The third corrector mirror (IM3), an off-axis segment of a reflective Schmidt plate, extends the correction over the 200" FOV. This mirror also folds the optical path toward the top of the optical bench, allowing easy inclusion of the filter wheel mechanisms and filters. This fold also positions the CCD closer to its radiative coolers, which shortens the length of the heat pipes.

The resultant image quality at the CCD surface is nearly uniform with field, and better than  $\lambda/20$  over the entire field. The design wavefront error varies from 0.015 to 0.051 waves rms at 632.8 nm over the field. When this nominal design value is error-budgeted with other expected wavefront errors due to manufacture, lack of flatness of the CCD photosensitive surface, and alignment, the overall wavefront error is estimated to be less than 0.079 waves rms at 632.8 nm in the worst case field position, which yields a diffraction-limited Strehl ratio of 80 percent. To achieve this performance within the OTA, focus and pupil alignment adjustment is required on orbit, as with COSTAR, STIS, and NICMOS. The tilt and focus range of the first corrector mirror alignment mechanism used on COSTAR, and duplicated on STIS and NICMOS, provides sufficient tilt and focus range to meet ACS requirements. Table 3 summarizes the error budgets for the three cameras.

Table 3: Wavefront errors (includes focus and alignment errors)

|                                   | (Waves RMS @ 632.8 nm) |        |                     |
|-----------------------------------|------------------------|--------|---------------------|
|                                   | WFC                    | HRC    | SBC                 |
| Predict                           | 0.079                  | 0.065  | 0.064               |
| Specification                     | <0.085                 | <0.085 | <0.085              |
| Goal                              | <0.075                 | <0.075 | <0.075              |
| L.O.S. Jitter (over 1300 seconds) |                        |        |                     |
| Predict                           | 2.62                   | 2.94   | 2.62 milli arc sec  |
| Specification                     | <3.0                   | <3.0   | <3.0 milli arc sec  |
| L.O.S. Drift (over 2 orbits)      |                        |        |                     |
| Predict                           | 8.5                    | 11.63  | 11.26 milli arc sec |
| Goal                              | <10.0                  | <10.0  | <10.0 milli arc sec |

### 2.2.2 The Wide Field Camera CCD Enclosure

The two WFC CCDs are mounted in a vacuum enclosure which is designed to isolate the CCDs from thermal radiation and contamination. Figure 6 shows a schematic of the enclosure. At the time of this writing we plan to cool the CCDs by using radiators to dissipate heat into the HST's aft shroud. The CCDs are cooled to -80°C by thermal electric coolers (TECs; mounted in the detector housings) that are thermally strapped to the radiators to dissipate their thermal load. As on STIS, each CCD detector can be heated for in-orbit annealing of any radiation induced damage by turning off the TECs. Because the aft shroud is warming at a rate of approximately 0.6 to 1°C per year as the reflectivity and emissivity of the HST exterior degrade, we may need to attach the heat straps to an external radiator.

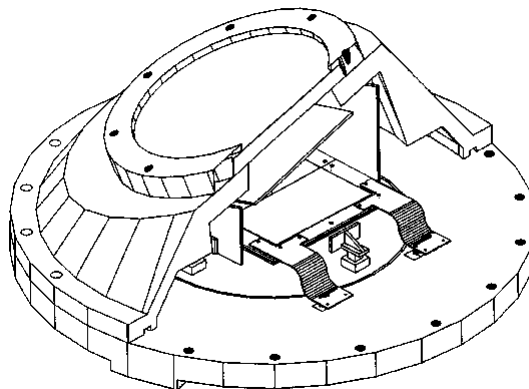


Fig. 6: Schematic of the WFC CCD housing

Each thinned WFC CCD is bonded to a soda glass die. The die is in turn bonded with indium solder to an AlN CCD carrier. Two CCD carriers are in turn soldered side by side to another AlN plate, the focal plane carrier. Finally, the focal plane carrier is attached to a single four-stage TEC. The entire assembly is enclosed in an evacuated housing which has been cleaned and baked at high temperature before sealing. The enclosure has an anti-reflection coated fused silica window at ambient temperature. The heat load on the large WFC CCD is reduced by a cooled inner enclosure and a second cooled anti-reflection coated fused silica window. The inner enclosure is cooled by four two-stage TECs.

### 2.3 The High Resolution Camera and Enclosure

The HRC provides spectral coverage from 200-1000 nm with a 26''x29'' arc sec field of view. The detector is a 1024x1024 STIS-like CCD manufactured by SITe. This CCD will be optimized for high quantum efficiency in the near-ultraviolet by Mike Lesser at the University of Arizona. Lesser's process uses a platinum flashgate (PPtF) and an AR coating optimized for the 200-300 nm bandpass. If Lesser's process is not perfected in time to meet the ACS schedule, we will use a SITe CCD with a new SITe ultraviolet anti-reflection coating. Figure 7 shows the QE expected from Lesser's process, the QE from the new SITe UV coating, and the QE of the STIS CCD. The net HRC plus HST OTA efficiency is shown in Figure 5.

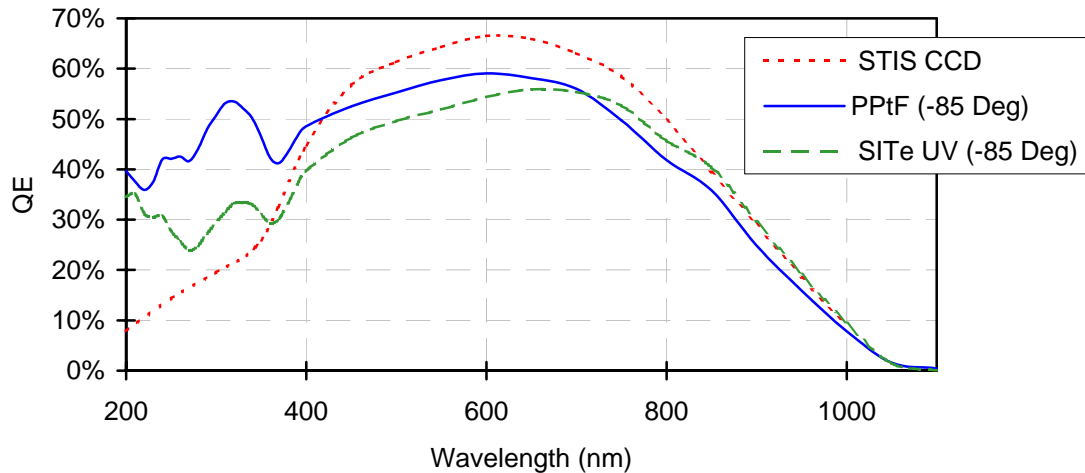


Fig. 7: Expected HRC QE with SITe's and Lesser's processes

The HRC CCD is mounted in a vacuum enclosure which is a STIS mechanical and thermal design. The single fused silica CCD detector window is oriented normal to the chief ray to minimize lateral color. The CCD is tilted to match the best image surface. The angle between the window and the CCD is 30.8 degrees.

#### 2.3.1 The High Resolution Camera Optics and Optical Performance

The HRC image is critically sampled for wavelengths greater than 500 nm, with an average plate scale of 0.025''/pixel. The HRC uses only two powered mirrors and a fold mirror to relay the HST field image to the CCD for highest throughput and lowest scatter.

The first two HRC mirrors (M1 and M2) are configured similarly to the first two WFC mirrors. The third mirror (M3), the flat HRC fold mirror which is on a two position mode selection mechanism, folds the optical path towards the top of the optical bench and aligns the chief ray parallel to that of the WFC so that the HRC and WFC can share the filter wheel mechanisms.

The HRC mirrors are coated with aluminum plus MgF<sub>2</sub> to achieve the highest possible reflectivity between 122 nm to 1000 nm. The coatings of the first two mirrors are optimized from Lyman-α longward. The third mirror coating is optimized from 200 nm longward. The first two mirrors are used at near normal incidence to minimize the polarization sensitivity. Including the fold mirror, which is used at 47.9 degree angle of incidence, this configuration yields only 1.0 percent degree of polarization sensitivity at 436 nm and 4.3 percent at the worst-case wavelength of 800 nm.

A full 26 by 29 arc sec FOV is available. The resultant image quality at the CCD surface is equal to or better than λ/20 everywhere. Residual aberrations are balanced to yield an optimum image over the HRC and the SBC FOV. The design wavefront error varies from 0.003 to 0.018 waves rms at 632.8 nm over the field. When this nominal design value is error-budgeted with other expected wavefront errors due to manufacture, CCD curvature, and alignment, the overall wavefront error is estimated to be less than 0.065 waves at 632.8 nm, which yields a high Strehl ratio of 82 percent.

As in the WFC, on-orbit focus and pupil alignment adjustment is required. This is accomplished by mounting the M1 mirror on a "Wally Wobbler", a novel mechanism which provides tip, tilt, and focus adjustment. This mechanism, designed by Wallace Meyers at the Ball Aerospace Corporation, incorporates three nested cylinders, driven by two motors (two degrees of freedom),

which rotate about axes which have a relative angle, with the axes meeting at the point of nutation. The Wobbler is best thought of in a spherical coordinate system, wherein the two degrees of freedom are the precession angles of the constant nutation angles, the outer nutation riding on the inner. The resultant pointing axis of the mechanism is in a conical range, and is the vector addition of the nutation vectors.

## 2.4 The Solar Blind Camera

The SBC is optimized for highest throughput from 115 nm to 170 nm. The image is sampled at 0.030"/pixel. The SBC uses a STIS-based PCA photon-counting detector with an opaque CsI photocathode and a C-plate micro-channel plate (MCP). The relay optics and corrector mirror mechanism are shared with the HRC camera. A full 26" by 29" FOV is available. The resultant image quality at the PCA MCP surface is better than  $\lambda/8$  everywhere in the FUV, and nearly uniform with field. The wavefront error varies from 0.016 to 0.123 waves rms at 143.5 nm over the field. The design is optimized from 121.6 to 160.8 nm. When operated monochromatically at different wavelengths within the CsI response, there is very little variation in the image. When operated broad band, some lateral color is evident in the image. For instance, the field-weighted rms wavefront error in waves at 632.8 nm is 0.0188 for an operational wavelength of 143.5 nm, 0.0184 for 121.6 nm, 0.0193 for 160.8 nm, and 0.0224 nm when operated broadband. The expected QE of the SBC detector, including the HST OTA, is shown in Figure 8.

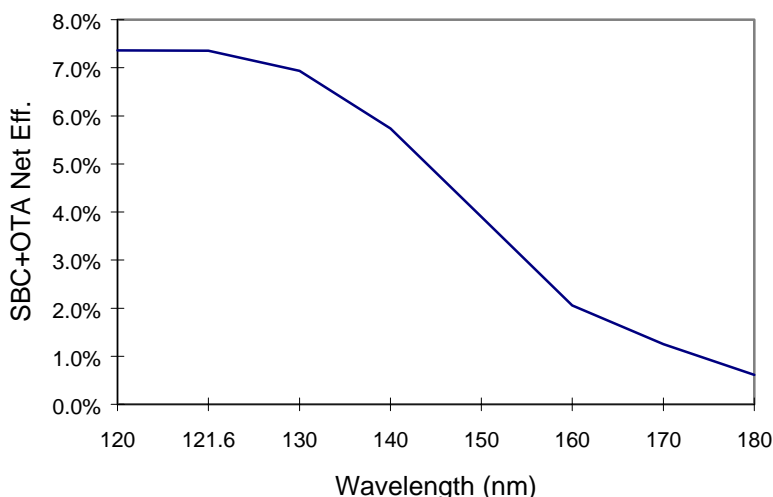


Fig. 8: Expected SBC net efficiency (including the HST OTA) versus wavelength

## 2.5 The Optical Bench and Mechanisms

The optical components, mechanisms, and detectors require critical alignment and therefore are mounted to a stable optical bench of near zero thermal expansion. The bench is kinematically isolated inside the enclosure to prevent thermally or structurally induced distortions from effecting optical alignment. The ACS enclosure latches to the OTA and supports the ACS electronics boxes. The optical bench and enclosure have strong heritage to GHRS, STIS, and NICMOS. The structural design of the optical bench is very similar to the STIS design and uses the same graphite/epoxy materials and lay-ups. The tubes are a hybrid laminate design using HMS1/3501-6 (fiber/resin) for the 0 degree plies and AS4/3501-6 for the 71 degree plies. All plate material is a quasi-isotropic laminate design made of UHMS/3501-6. The CTE design requirement of  $0.0 \pm 0.09 \times 10^{-6}$  per degree C has been demonstrated on the STIS bench and also meets the requirements for the ACS optical bench.

Table 4 lists the mechanisms for ACS and describes their functions. Three filter wheels are provided; two are shared by the WFC and HRC and the third is dedicated to the SBC. If the PCA detects an out of limits exposure the SBC filter wheel provides bright object protection by quickly rotating to one of the opaque filter wheel positions which alternate with the filters. The HRC fold mirror mechanism is used to select either the HRC or SBC. When it positions the M3 mirror into the optical path, the light is reflected to the HRC CCD. When the mirror is in the down position the M3 mirror is removed from the optical path and the light passes directly to the SBC PCA. A calibration door serves three functions. The door can be closed to prevent light from either entering or escaping the ACS. When the door is enclosed, a diffuser attached to the door reflects light from the calibration sources into the three cameras. Finally, the calibration door has an intermediate position which inserts the

coronagraph into the optical path of the HRC (c.f. section 4). Each CCD has a dedicated shutter that determines the exposure time. These mechanisms have a high level of heritage with STIS and CO-STAR.

Table 4: ACS Mechanisms and Their Functions

| Mechanism                             | Functions   |
|---------------------------------------|---|
| WFC/HRC filter wheel #1 (Lower Wheel) | Select optic on filter wheel for WFC and HRC  |
| WFC/HRC filter wheel #2               | Select optic on filter wheel for WFC and HRC  |
| SBC filter wheel                      | Select optic on filter wheel for SBC<br>Provide bright object procession for the SBC  |
| HRC fold mirror                       | Reflect field of view to the HRC CCD<br>Remove (down) when SBC used<br>Up to protect the SBC when the SBC filter wheel is rotated |
| WFC corrector (Focus and Tip/Tilt)    | Alignment for aberration correction of the WFC  |
| HRC corrector (Focus and Tip/Tilt)    | Alignment for aberration correction of HRC/SBC  |
| Calibration door                      | Prevent external input during in-flight calibration<br>Position diffusers in calibration path                                     |
| WFC CCD shutter                       | Shutter the WFC CCD   |
| HRC CCD shutter                       | Shutter the HRC CCD   |

### 3. FILTERS AND DISPERSERS

We have simplified the optical design and reduced cost by sharing the filter wheels for the WFC and HRC, as well as sharing the corrector optical path for the HRC and SBC. The WFC and HRC filter wheel mechanism is comprised of two separate filter wheels, each driven by an independent motor and sharing a common housing. These filter wheels are populated with 17 bandpass filters (13 of which are spectrally compatible with both the WFC and HRC), a set of five linear ramp filters, a grism for the WFC, and a prism and three visible and three ultraviolet polarizers for the HRC. The SBC has five longpass filters, two prisms, a narrow band Lyman- $\alpha$  filter, and four opaque positions. Altogether ACS incorporates a total of 38 spectral elements. The respective diameters of the WFC and HRC filters are 86.6 mm and 38.1 mm in diameter. The large WFC filters can be used with the HRC. Figure 9 shows the bandpasses of the filters. Seven filters are allocated to broad band imaging in the visible and near UV. The primary filters are based on the Sloan Digital Sky Survey filter set, where we include the u, g, r, i, and z bands. Two near-UV filters are similar to the F218W and F255W filters currently in the WFPC2 and provide continuity between the two instruments. These will be complemented by one set of broad band U, B, V, and I filters, also similar to the current WFPC2 filters, for wide-field imaging surveys. The I-band filter (close to F814W), in particular, will be designed to cover a wide bandpass for deep surveys.

Narrow band filters for the WFC and HRC take three forms: standard narrowband filters which cover the whole field of view of both cameras, linear ramp filters similar in concept to those on WFPC2, and an HRC methane band filter for observations of the giant planets. The standard narrowband filter complement is H $\alpha$ , [O III] and [Ne V]. In order to satisfy our own scientific goals and to provide a new capability for the community, we have included a set of four narrow band (~2%) and one broad band (~9%) linear ramp filters to provide an imaging capability for redshifted emission line sources. The ramp filters cover the wavelength region from approximately 370 nm to 1050 nm. Each of the narrow band ramp filters covers a wavelength range of approximately 100 nm, split up into 50 nm per strip. The filter designs ensure continuous wavelength coverage from one strip to the next and no loss of coverage from vignetting near the edge of the field of view. The desired bandpass is selected by a combination of target positioning and filter wheel rotation. The central strip of each of the five linear ramp filters can be used with the HRC. Two sets of polarizers, one for the UV and the other for the visible, also are included for imaging with the HRC: the UV set is on filter wheel #1 for use with the HRC UV filters on filter wheel #2; the visible set is on filter wheel # 2 for use with the WFC broad band and narrow band filters on filter wheel #1. Each set of polarizers consists of three separate elements to give relative polarizing angles of 0, 60, and 120 degrees. Each polarizer must be used in conjunction with an additional filter in order to maintain focus. The spectral range of the polarizers is 250 nm to 700 nm for the UV and 450 nm to 800 nm for the visible polarizers.

The SBC filter wheel contains a set of short-cut filters which step across the SBC bandpass. The broadest filter, MgF<sub>2</sub>, transmits geocoronal Lyman- $\alpha$ . The filter with the second largest bandpass, CaF<sub>2</sub>, blocks geocoronal Lyman- $\alpha$  and transmits light longward of 125 nm. We have included a relatively narrowband Lyman- $\alpha$  filter for observations of auroras on the outer planets.

The ACS includes three prisms and a grism for deep, low spectral resolution imaging from 120 nm to 1000 nm. We use a grism with a resolution of 100 in the large format WFC. The first order spectrum extends from 550 nm to the WFC CCD cutoff at  $\sim$ 1100 nm. Second order blue and yellow light are blocked by combining the grism with a 550 nm longpass substrate. The dispersing element for the HRC is a Sapphire prism which gives high transmission and good dispersion in the spectral region from 200 to 400 nm. The spectral resolving power of  $R \sim 100$  at 200 nm gives a very faint limiting magnitude. The dispersing elements for the SBC will be a lithium fluoride (LiF) prism and a calcium fluoride (CaF<sub>2</sub>) prism. LiF provides high transmission, high efficiency (no light in zero and high orders), and relatively constant dispersion from 120 to 180 nm. The prism is designed to give a resolving power of 100 at 142 nm. The CaF<sub>2</sub> ( $R \sim 100$  at 150 nm) prism begins transmitting at  $\sim$  125 nm, and is included for observations where it is desirable to block geocoronal Lyman- $\alpha$ .

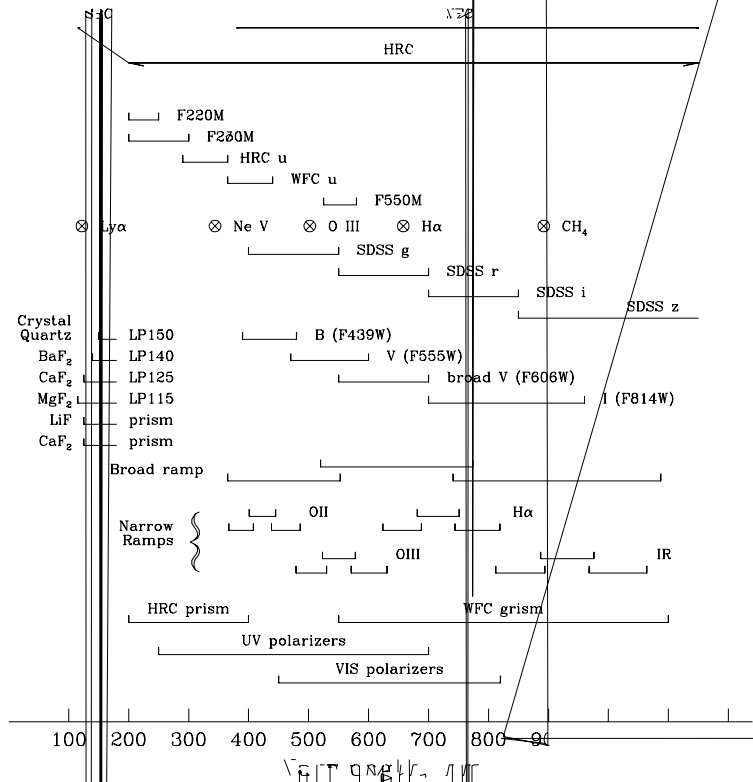


Fig. 9: ACS filter summary. The wavelength range covered by each channel is indicated at the top of the chart. The horizontal bars represent the bandpass of each filter; the filter's name is given at the right hand side of the bandpass. The narrow band ( $\sim$ 1%) filters are shown by a "⊗" symbol with the name of the emission line next to it. A set of broad band filters similar to the ones currently used in WFPC2 (names in parentheses) provide continuity between the two instruments and a clean transformation to the classical Johnson and Cousins systems. The ACS is equipped with a set of narrow ( $\sim$ 2%) ramp filters for emission-line imaging of redshifted objects. A broad ( $\sim$ 9%) ramp filter is also included for off-band continuum imaging. Dispersing elements include two prisms for the SBC, one for HRC, and a grism for WFC.

**4. CORONAGRAPH**

The ACS coronagraph will have two high contrast options. Both options provide for suppression of the light from a bright object which is positioned behind a mask using autonomous on-board target acquisition. These options will be used for the observation of quasar host galaxies, circum-nuclear regions in active galactic nuclei, stellar disks and outflows, protostellar disks and jets, and some planetary observations such as the Io torus. They can also be used in searches for substellar companions to nearby stars.

The first option is a "Fastie spot", which is a 0.8 arc second diameter reflecting spot deposited near the corner of the HRC CCD entrance window (where the beam size is 0.5 arc seconds). It will allow unvignetted high contrast imaging (including with the ramp filters) from 0.7 to 4 arc seconds around a bright source (for example imaging of a quasar host galaxy.) Vignetted, but still useful data will be available all the way in to 0.4 arc seconds from the source. The full CCD field will also be available so by

viewing at four different position angles; a field width of 44 arc seconds is available. The spot does not significantly reduce the level of diffracted light in the wings of a bright point source positioned behind it, but by preventing the light from crossing the window and hitting the CCD, instrumental scatter, ghosts, and CCD bleeding will be minimized. These effects raise the point spread function (PSF) wings by almost an order of magnitude in WFPC2, which does not have such a facility.

The second option is a commandable coronagraphic mask that can be positioned in the aberrated HST focal plane, together with a Lyot stop that is simultaneously positioned at the pupil image close to the M2 mirror. This option does not interfere with normal camera operation in any way. The coronagraphic mask consists of two stops each with a smoothly graded edge. One is positioned near the circle of least confusion in the center of the aberrated HRC field of view and has a radius of 0.9 arc seconds. The second is designed for the brightest targets and has a radius of 1.5 arc seconds (and a graded edge). It is positioned directly over the Fastie spot. The masks are positioned in such a way that the center wavelength in the linear ramp filters for each is the same, so observations with both can be made without repositioning the filter wheel. The Lyot stop has the effect of removing the diffracted light halo that surrounds the target, giving almost an order of magnitude higher contrast improvement at the longest wavelengths. The expected performance from these high contrast options is shown in Figure 10. The residual halo that is present is caused by scatter from ripples in the primary and secondary mirrors.

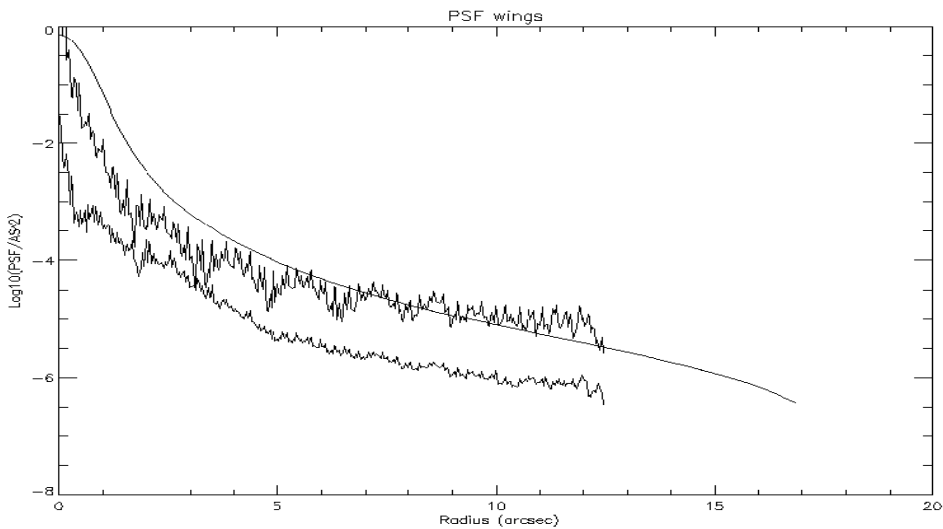


Fig. 10: The smooth curve is the PSF for a 2.4-m telescope with 1" seeing. The middle curve is the expected ACS PSF. The bottom curve shows the expected PSF with the ACS coronagraph.

## 5. OPERATIONAL MODES

Two major operational features of the ACS improve its science productivity and provide efficient operation. The first feature allows the observer to simultaneously use two cameras for parallel imaging. This is made possible by two filter wheels (shared by the WFC and HRC for cost savings reasons), containing a total of 30 filter positions, each of which can be used by the WFC and HRC, and a third 12-position filter wheel dedicated to the SBC. The WFC/HRC filter wheels are rather large (0.6 m diameter) and are driven by redundant stepper motors at 0.75 rpm.

The second feature allows simple WFPC2-like target acquisition because the fields of view of each camera are large compared to HST pointing uncertainties. Additionally, although each optical channel of the Advanced Camera is optimized for specific types of science, a number of operational features have been designed into the ACS to allow the observer to select permitted combinations of optical channels, to choose a particular readout mode, and to configure filter elements to enhance their specific science programs. For example, the large format and layout of the WFC CCD's make it particularly well suited for large-scale, deep mapping surveys, by making it possible to obtain contiguous exposures with single guide star acquisitions. The rows and columns of the WFC and HRC CCDs are parallel to the V2 and V3 axes, making it possible to efficiently "tile" a survey area while stepping the guide stars along the long directions of the FGS sensors.

The major operating modes of the ACS are described below.

Direct *Full-Frame Imaging* with any of the three cameras is the primary science operational mode. For this mode, no binning of the data is provided for the CCD's or the SBC detectors. Also the SBC will routinely image at 1024×1024 (low resolution). Imaging may be carried out with the filters described in section 3.

*Postage Stamp Imaging Mode* may be implemented by a user specified  $n \times m$  array on either of the CCD's. No postage stamp imaging is provided for the SBC. One rectangular sub array may be specified (one column or row away from edges and not across the WFC chip boundary) and only the data from that portion of the detector will be stored in buffer memory. Fast data transfer from the CCD occurs in areas not included within the specified sub array, thus yielding a more rapid readout and (depending on sub array size), hence increased time resolution. In addition to faster readout times, which permit more rapid observing sequences, this mode enables storage of a greater number of frames in the image buffer. Although our proposed science program does not require time resolution greater than that provided by normal CCD operations, this capability will increase the time resolution when used as a *Time Resolved Mode*.

As already noted, a major operational feature of the ACS is its ability to use two detector channels for *Parallel-Full Frame Imaging* to provide simultaneous exposures. To fully use the discovery potential of the WFC channel, the WFC will be used in parallel with the HRC or SBC whenever these channels are performing prime science observations. When the WFC is prime, either the HRC or SBC may be used in parallel, the choice depending on the specific science program. When the HRC is prime, only the WFC may be operated in parallel due to the optical configuration of the ACS. We expect that this option will be used most frequently due to its high DQE. When the SBC is prime, again only the WFC may be operated in parallel, or not, depending on the observer's science program. Filters for each channel are user-specified although there are some restrictions on filter combinations for parallel observations. Although the filter locations and the order of the filters on the WFC and HRC filter wheels have been optimized for simultaneous use of the two cameras, the filter pairings are complicated by the packaging of the filter wheels in the optical bench, by the individual filter designs which are parfocalized, by the filter construction (the ramp filters are built in three sections), and by the differing sizes of the HRC (small) and WFC (large) filters on each wheel for each CCD detector. Parallel operations are completely deterministic in the sense that when a filter is chosen for the prime camera (WFC or HRC), the filter for the parallel camera (HRC or WFC) is automatically determined. Since the chief rays for the two cameras are separated on the two filter wheels by 153.5 degrees, rather than 180 degrees (also due to packaging constraints within the ACS optical bench), there are, consequently, a limited number of filters for each camera that will have a corresponding single filter path to the other camera.

Although simultaneous integrations are possible, flight software limitations require sequential readouts and data transfer to the Science Data Formatter.

We expect the WFC to be used extensively for parallel serendipitous survey work when other scientific instruments are prime.

As described in section 4, the Advanced Camera also includes a *Coronagraphic Mode* consisting of two independent coronagraphs: (1) a Fastie Spot Coronagraph, and (2) an Aberrated Beam Coronagraph.

Finally, the ACS optical design includes a set of internal continuum source lamps that cover the full spectral range of the CCD cameras and a portion of the SBC camera for an *Internal Calibration Mode*. Tungsten lamps provide complete spectral coverage for the WFC: Tungsten and Deuterium lamps give spectral coverage for the HRC; and Deuterium covers the SBC spectral response. These lamps provide illumination into each of the camera channels by deploying the aperture door mechanism in the closed position. The light from the lamps is then scattered by a diffuser on the inside of the calibration door into the optical path for each channel and uniformly illuminates the detectors. This door also isolates the instrument from the HST/OTA hub, and is fully redundant to avoid the possibility of single point failure. The door can also be used to augment bright object protection and ensures that no stray light from the ACS during calibration will affect the other scientific instruments. These internal calibration lamps will be used periodically to obtain flat field (sensitivity variations as a function of position on the detector) calibration reference files.

## 6. THE SCIENCE PROGRAM

We plan to use the unique characteristics and dramatically improved efficiencies of the ACS for a focused attack on three major science themes. The WFC and HRC will address the formation and evolution of galaxies and clusters of galaxies, and the nature and large-scale distribution of dark matter. We will devote approximately 75 percent of our guaranteed time to two major surveys aimed at solving outstanding problems in cosmology.

In the largest survey we will take contiguous deep V- and I-band WFC images of  $\sim 0.7$  square degrees of sky in the CVZ. We expect to use gravitational lensing of background galaxies to map the large-scale distribution of dark matter around approximately 20 rich clusters of galaxies. The survey data will establish the evolution of galaxies and clusters of galaxies in the early universe and determine the cluster and supercluster environment around one or more high redshift radio galaxies.

In the second survey, we will use Surface Brightness Fluctuations (SBF) in deep WFC I-band images of early type galaxies to map large-scale flow. This method will allow us to obtain distances to galaxies which are independent of their redshifts and will contribute to the measurement of  $H_0$  and to the mapping of large-scale flows. Mapping the infall pattern around the "Great Wall" of galaxies will provide us with constraints on the mass distribution on very large-scales, which is presumably dominated by dark matter dynamics.

We will use narrow band and polarimetric HRC and WFC images to study QSOs and AGNs, our second major science area. These objects are not only unique probes of early universe conditions and potential tracers of the geometric evolution of the universe, but also are important for establishing the characteristics of nuclear engines. Our observations of AGNs will delineate the structure in the Narrow Line Region of AGNs and provide morphological data on stellar populations and related ionized gas. HRC observations will elaborate on the relationship between the host galaxies and associated radio sources. Imaging polarimetry data will be used to study proposed Unified Schemes for understanding active galaxies. We will use a novel polarimetric technique to measure the geometric distances to galaxies, and provide a new means to measure  $H_0$  and  $q_0$ . The coronagraph will be used to study the narrow line regions close the nuclei of active galaxies and the host galaxies of quasars. We will use the coronagraph to search nearby stars for proto-planetary disks, brown dwarf companions, and planets.

Finally, a variety of observations using narrow band imaging with the SBC will address specific questions in solar system science, our third science theme. The SBC will provide high spatial resolution narrow band data on auroras of the giant planets.

## 7. ACKNOWLEDGMENTS

The Advanced Camera is funded by NASA through the HST Project Office at the Goddard Space Flight Center.